Designation: E 598 – 96 (Reapproved 2002)

Standard Test Method for Measuring Extreme Heat-Transfer Rates from High-Energy Environments Using a Transient, Null-Point Calorimeter[1]

This standard is issued under the fixed designation E 598; the number immediately following the designation indicates the year of original adoption or, in the case of revision, the year of last revision. A number in parentheses indicates the year of last reapproval. A superscript epsilon (ε) indicates an editorial change since the last revision or reapproval.

1. Scope

1.1 This test method covers the measurement of the heat-transfer rate or the heat flux to the surface of a solid body (test sample) using the measured transient temperature rise of a thermocouple located at the null point of a calorimeter that is installed in the body and is configured to simulate a semi-infinite solid. By definition the null point is a unique position on the axial centerline of a disturbed body which experiences the same transient temperature history as that on the surface of a solid body in the absence of the physical disturbance (hole) for the same heat-flux input.

1.2 Null-point calorimeters have been used to measure high convective or radiant heat-transfer rates to bodies immersed in both flowing and static environments of air, nitrogen, carbon dioxide, helium, hydrogen, and mixtures of these and other gases. Flow velocities have ranged from zero (static) through subsonic to hypersonic, total flow enthalpies from 1.16 to greater than 4.65×10^1 MJ/kg (5×10^2 to greater than 2×10^4 Btu/lb.), and body pressures from 10^5 to greater than 1.5×10^7 Pa (atmospheric to greater than 1.5×10^2 atm). Measured heat-transfer rates have ranged from 5.68 to 2.84×10^2 MW/m^2 (5×10^2 to 2.5×10^4 Btu/ft^2-sec).

1.3 The most common use of null-point calorimeters is to measure heat-transfer rates at the stagnation point of a solid body that is immersed in a high pressure, high enthalpy flowing gas stream, with the body axis usually oriented parallel to the flow axis (zero angle-of-attack). Use of null-point calorimeters at off-stagnation point locations and for angle-of-attack testing may pose special problems of calorimeter design and data interpretation.

1.4 *This standard does not purport to address all of the safety concerns, if any, associated with its use. It is the responsibility of the user of this standard to establish appropriate safety and health practices and determine the applicability of regulatory limitations prior to use.*

2. Referenced Documents

2.1 *ASTM Standards:*

E 422 Test Method for Measuring Heat Flux Using a Water-Cooled Calorimeter[2]

E 511 Test Method for Measuring Heat Flux Using a Copper-Constantan Circular Foil, Heat-Flux Gage[2]

3. Terminology

3.1 *Symbols:*

a = Radius of null-point cavity, m (in.)
b = Distance from front surface of null-point calorimeter to the null-point cavity, m (in.)
C_p = Specific heat capacity, J/kg–K (Btu/lb-°F)
d = Diameter of null-point cavity, m (in.)
k = Thermal conductivity, W/m–K (Btu/in.-sec-°F)
L = Length of null-point calorimeter, m (in.)
q = Calculated or measured heat flux or heat-transfer-rate, W/m^2 (Btu/ft^2-sec)
q_0 = Constant heat flux or heat-transfer-rate, W/m^2 (Btu/ft^2-sec)
R = Radial distance from axial centerline of TRAX analytical model, m (in.)
r = Radial distance from axial centerline of null-point cavity, m (in.)
T = Temperature, K (°F)
T_b = Temperature on axial centerline of null point, K (°F)
T_s = Temperature on surface of null-point calorimeter, K (°F)
t = Time, sec
Z = Distance in axial direction of TRAX analytical model, m (in.)
α = Thermal diffusivity, m^2/sec (in.^{2}/sec)
ρ = Density, kg/m^3 (lb/in.^{3})

4. History of Test Method

4.1 From literature reviews it appears that Masters and Stein **(1)**[3] were the first to document the results of an analytical study of the temperature effects of axial cavities drilled from the backside of a wall which is heated on the front surface (see Fig. 1). These investigators were primarily concerned with the deviation of the temperature measured in the bottom of the

[1] This test method is under the jurisdiction of ASTM Committee E21 on Space Simulation and Applications of Space Technology and is the direct responsibility of Subcommittee E21.08 on Thermal Protection.

Current edition approved Oct. 10, 1996. Published December 1996. Originally published as E 598 – 77. Last previous edition E 598 – 77 (1990).ε1

[2] *Annual Book of ASTM Standards*, Vol 15.03.

[3] The boldface numbers in parentheses refer to the list of references at the end of this test method.

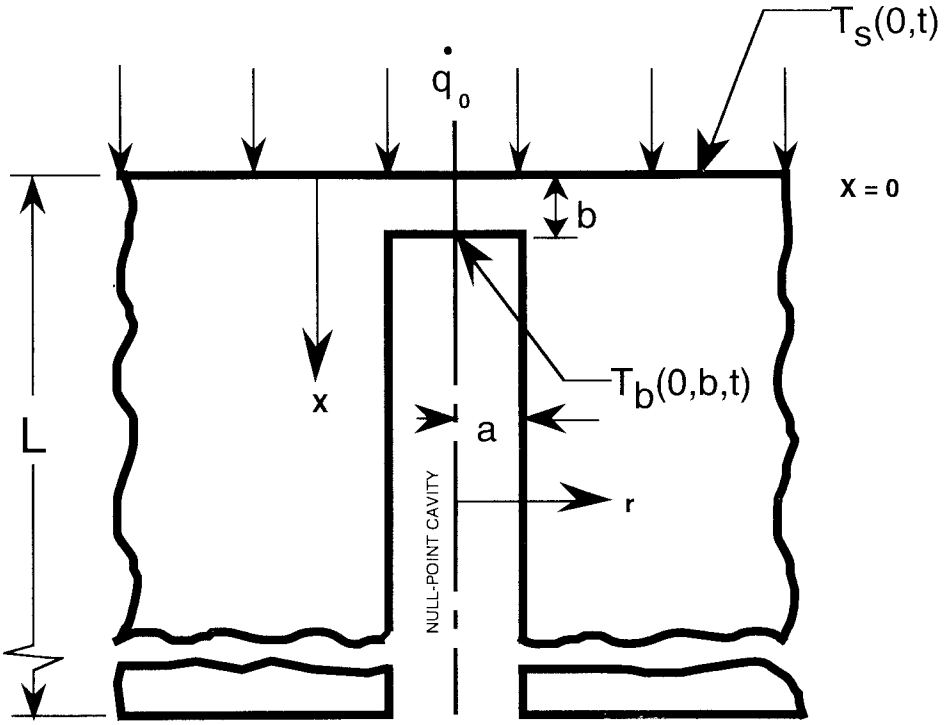

NOTE 1—1-T_s (0,t) = Surface temperature (x = 0) of a solid, semi-infinite slab at some time, t.
NOTE 2—2-T_b (0,b,t) = Temperature at r = 0, x = b of a slab with a cylindrical cavity at some time, t, heat flux, q, the same in both cases.

FIG. 1 Semi-infinite Slab with Cylindrical Cavity

cavity from the undisturbed temperature on the heated surface. Since they were not in possession of either the computing power or the numerical heat conduction codes now available to the analyst, Masters and Stein performed a rigorous mathematical treatment of the deviation of the transient temperature, T_b, on the bottom centerline of the cavity of radius, *a*, and thickness, *b*, from the surface temperature T_s. The results of Masters and Stein indicated that the error in temperature measurement on the bottom centerline of the cavity would decrease with increasing values of *a/b* and also decrease with increasing values of the dimensionless time, $\alpha t/b^2$, where α is the thermal diffusity of the wall material. They also concluded that the most important factor in the error in temperature measurement was the ratio *a/b*and the error was independent of the level of heat flux. The conclusions of Masters and Stein may appear to be somewhat elementary compared with our knowledge of the null-point concept today. However, the identification and documentation of the measurement concept was a major step in leading others to adapt this concept to the transient measurement of high heat fluxes in ground test facilities.

4.2 Beck and Hurwicz **(2)** expanded the analysis of Masters and Stein to include steady-state solutions and were the first to label the method of measurement "the null-point concept." They effectively used a digital computer to generate relatively large quantities of analytical data from numerical methods. Beck and Hurwicz computed errors due to relatively large thermocouple wires in the axial cavity and were able to suggest that the optimum placement of the thermocouple in the cavity occurred when the ratio *a/b* was equal to 1.1. However, their analysis like that of Masters and Stein was only concerned with the deviation of the temperature in the axial cavity and did not address the error in measured heat flux.

4.3 Howey and DeCristina **(3)** were the first to perform an actual thermal analysis of this measurement concept. Although the explanation of modeling techniques is somewhat ambiguous in their paper, it is obvious that they used a finite element, two dimensional axisymmetric model to produce temperature profiles in a geometry simulating the null-point calorimeter. Temperature histories at time intervals down to 0.010 sec were obtained for a high heat-flux level on the surface of the analytical model. Although the analytical results are not presented in a format which would help the user/designer optimize the sensor design, the authors did make significant general conclusions about null point calorimeters. These include: (*1*) "..., thermocouple outputs can yield deceivingly fast response rates and erroneously high heating rates (+ 18 %) when misused in inverse one-dimensional conduction solutions." (*2*) "The prime reason for holding the thermocouple depth at $R/E = 1.1$ is to maximize thermocouple response at high heating rates for the minimum cavity depth..." (Note: *R* and *E* as used by Howey and DeChristina are the same terms as *a* and *b* which are defined in 4.1 and are used throughout this document.) (*3*) A finite length null-point calorimeter body may be considered semi-infinite for:

$$\frac{(\alpha t)}{L^2} \leq 0.3$$

4.4 Powers, Kennedy, and Rindal **(4** and **5)** were the first to document using null point calorimeters in the swept mode. This method which is now used in almost all arc facilities has

the advantages of (*1*) measuring the radial distributions across the arc jet, and (*2*) preserving the probe/sensor structural integrity for repeated measurements. This technique involves sweeping the probe/sensor through the arc-heated flow field at a rate slow enough to allow the sensor to make accurate measurements, yet fast enough to prevent model ablation.

4.4.1 Following the pattern of Howey and DiCristina, Powers et. al. stressed the importance of performing thermal analyses to "characterize the response of a typical real null point calorimeter to individually assess a variety of potential errors, ...". Powers et. al. complain that Howey & DiCristina "... report substantial errors in some cases, but present no generalized results or design guide lines." They state concerning the analyses performed to support their own documentation, "In order to establish guidelines for null point calorimeter design and data reduction, analyses were performed to individually assess the measurement errors associated with a variety of non-ideal aspects of actual calorimeters." The conclusions reached from the results of the thermal analyses were broken down into eight sub headings and were discussed individually. Some of the conclusions reached were rather elementary and were previously reported in Refs **(1-3)**. Others were somewhat arbitrary and were stated without substantiating data. One specific conclusion concerns the ratio of the null-point cavity radius, *a*, to the cavity thickness, *b*. While stating that the optimum condition occurred when $a = b$, the authors of Ref **(4)** further state that when $a = 0.305$ mm (0.012 in.) and $b = 0.127$ mm (0.005 in.); $a/b = 2.4$, the calculated heat flux will be 20 % higher than the actual heat flux. In more recent documentation using more accurate and sophisticated heat conduction computer codes as well as an established numerical inverse heat conduction equation **(6)**, the error in indicated heat flux is shown to be considerably higher than 20 % and is highly time dependent.

4.5 The latest and most comprehensive thermal analysis of the null-point calorimeter concept was performed by Kidd and documented in Refs **(6** and **7)**. This analytical work was accomplished by using a finite element axisymmetric heat conduction code **(7)**. The finite element model simulating the null-point calorimeter system is comprised of 793 finite elements and 879 nodal points and is shown in block diagram form in Fig. 2. Timewise results of normalized heat flux for different physical dimensional parameters (ratios of *a* to *b*) are graphically illustrated on Figs. 3 and 4. The optimum value of the ratio *a/b* is defined to be that number which yields the fastest time response to a step heat-flux input and maintains a constant value of indicated $\dot{q}$/input $\dot{q}$ after the initial time response period. From Figs. 3 and 4, it can be seen that this optimum value is about 1.4 for two families of curves for which the cavity radius, *a*, is held constant while the cavity thickness, *b*, is varied to span a wide range of the ratio *a/b*. This is a slightly higher value than reported by earlier analysts. It is important to note that the analytical results do not necessarily have to give a value of indicated $\dot{q}$/input $\dot{q} = 1.0$ since this

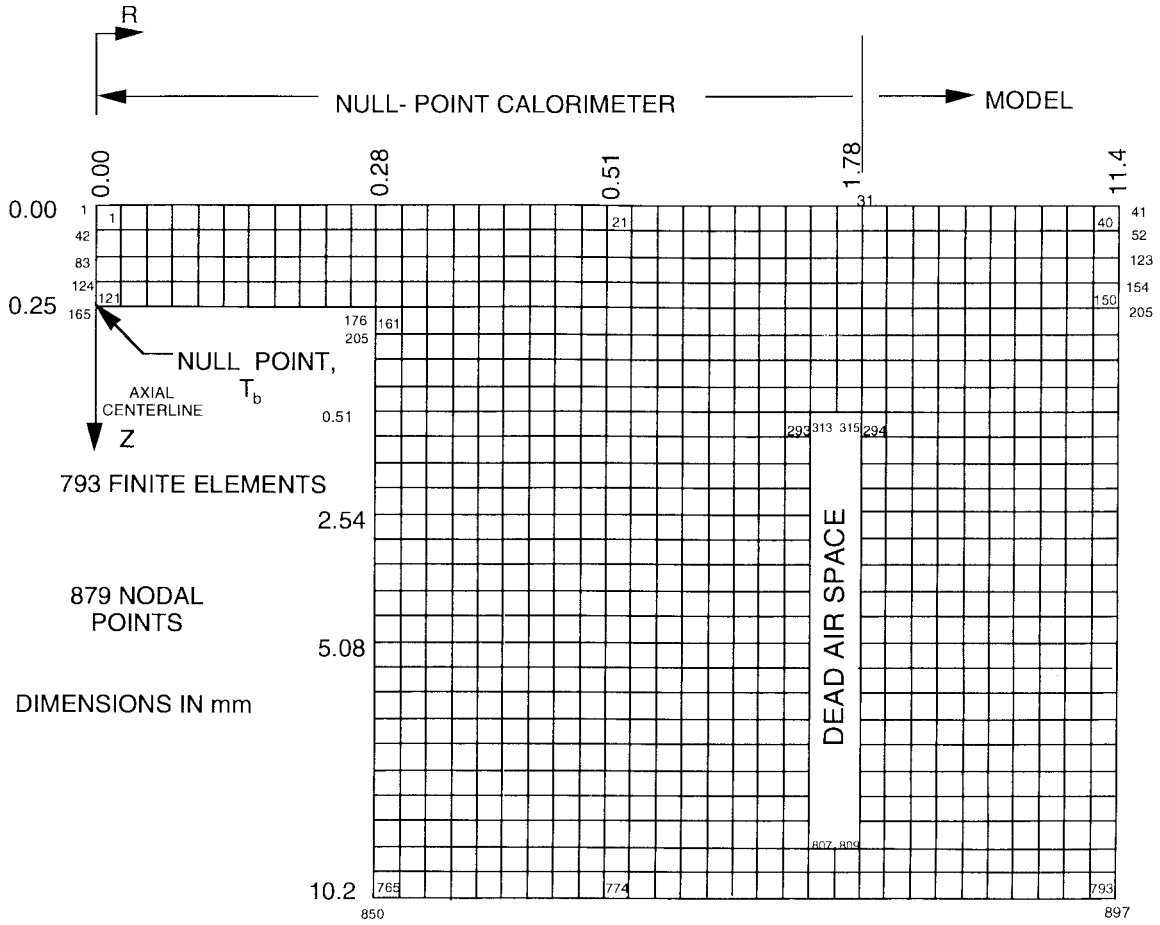

FIG. 2 Finite Element Model of Null-Point Calorimeter

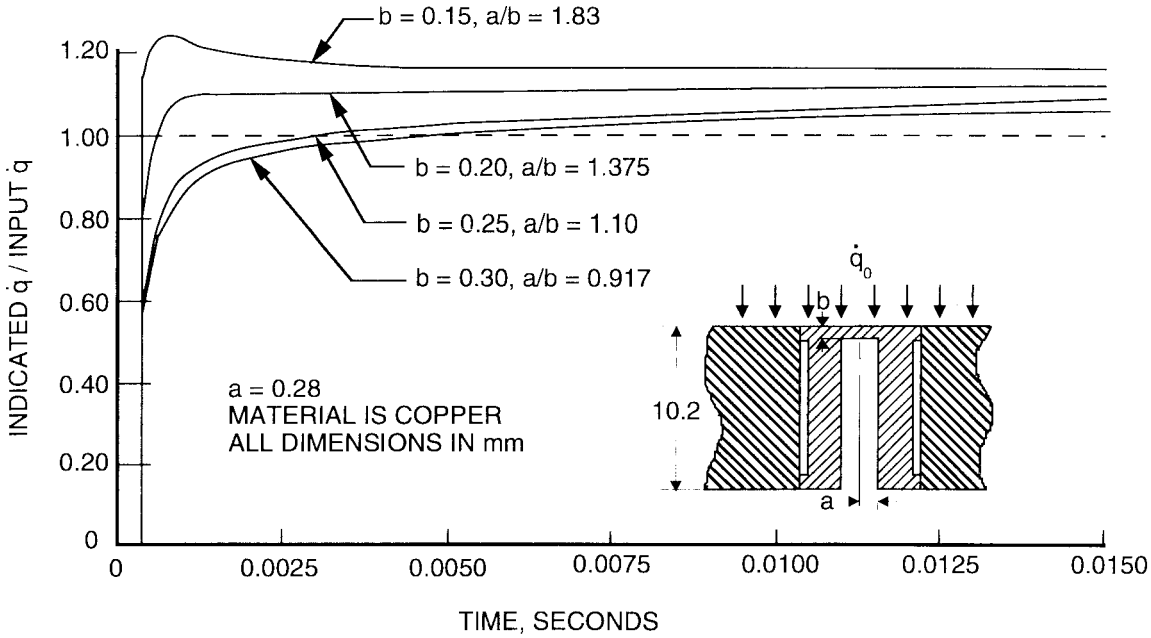

FIG. 3 Null-Point Calorimeter Analytical Time Response Data

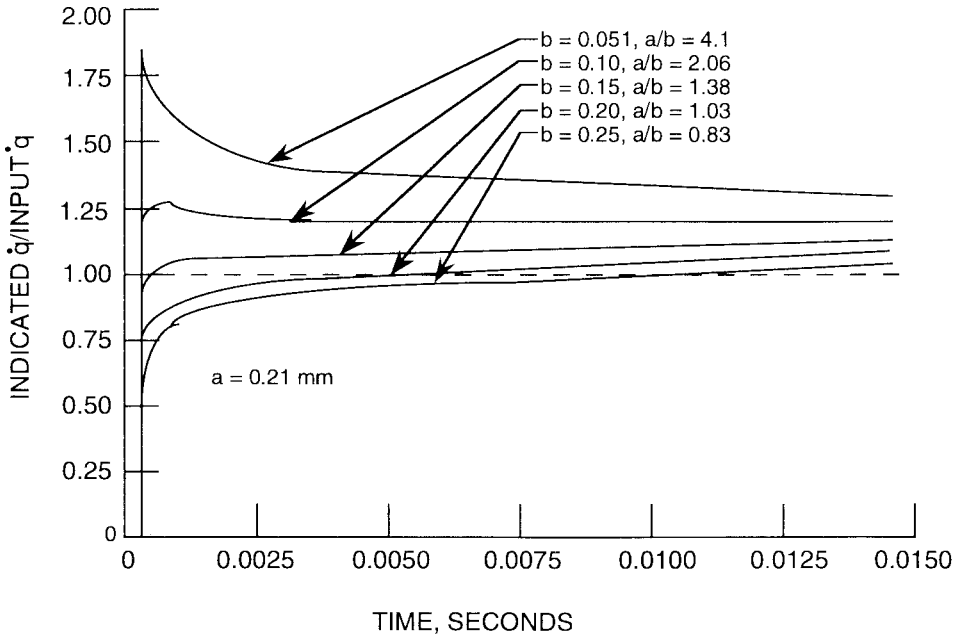

FIG. 4 Null-Point Calorimeter Analytical Time Response Data

difference can be calibrated in the laboratory. The data graphically illustrated on Figs. 3 and 4 and substantiate conclusions drawn by the authors of Refs **(3** nd **4)** that the calculated heat flux can be considerably higher than the actual input heat flux—especially as the ratio of *a/b* is raised consistently above 1.5. All of the users of null-point calorimeters assume that the device simulates a semi-infinite body in the time period of interest. Therefore, the sensor is subject to the finite body length, L, defined by $L/(\alpha t)^{1/2} \leq 1.8$ in order that the error in indicated heat flux does not exceed one percent **(6** and **7)**. This restriction agrees well with the earlier work of Howey and DiCristina **(3)**.

4.6 A section view sketch of a typical null-point calorimeter showing all important components and the physical configuration of the sensor is shown in Fig. 5. The outside diameter is 2.36 mm (0.093 in.), the length is 10.2 mm (0.40 in.), and the body material is oxygen-free high conductivity (OFHC) copper. Temperature at the null point is measured by a 0.508 mm (0.020 in.) diam American National Standards Association (ANSI) type K stainless steel-sheathed thermocouple with 0.102 mm (0.004 in.) diam thermoelements. Although no thermocouple attachment is shown, it is assumed that the individual thermocouple wires are in perfect contact with the backside of the cavity and present no added thermal mass to the system. Details of installing thermocouples in the null point cavity and making a proper attachment of the thermocouple

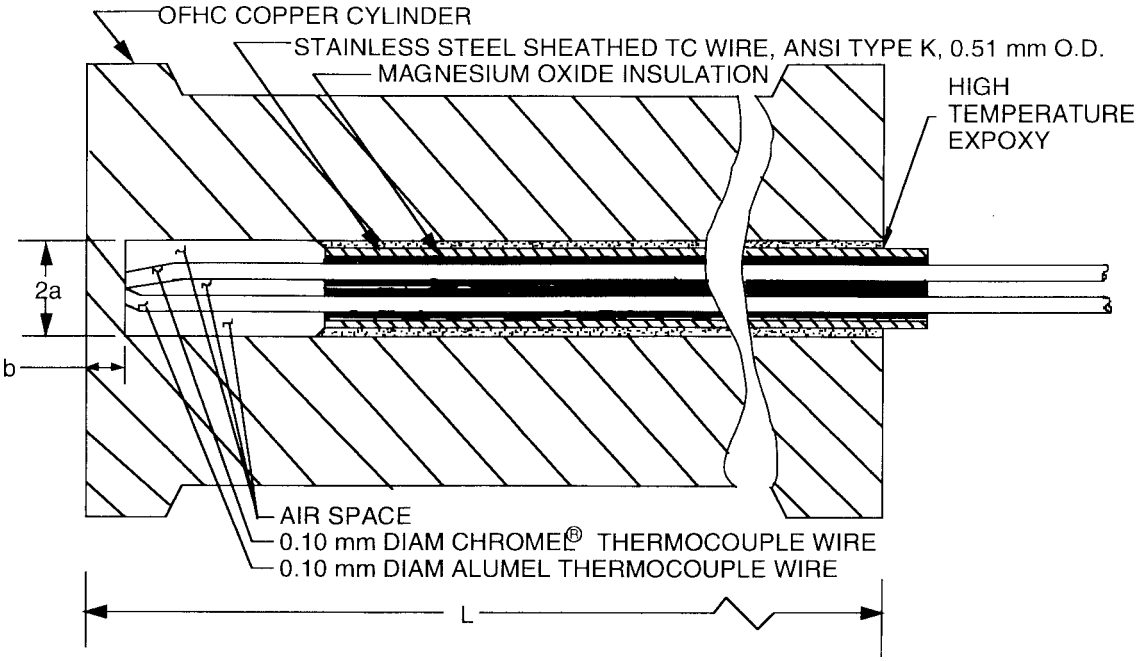

FIG. 5 Section View Sketch of Null-Point Calorimeter

with the copper slug are generally considered to be proprietary by the sensor manufacturers. Kidd in Ref **(7)** states that the attachment is made by thermal fusion without the addition of foreign materials. Note that the null-point body has a small flange at the front and back which creates an effective dead air space along the length of the cylinder to enhance one-dimensional heat conduction and prevent radial conduction. For aerodynamic heat-transfer measurements, the null-point sensors are generally pressed into the stagnation position of a sphere cone model of the same material (OFHC copper).

4.7 The value of the lumped thermal parameter of copper is not a strong function of temperature. In fact, the value of $(\rho C_p k)^{1/2}$ for OFHC copper varies less than three percent from room temperature to the melting point, 1356 K (1981°F); (see Fig. 6). Thermal properties of OFHC copper are well documented and data from different sources are in good agreement **(8)**. Most experimenters use the room temperature value of the parameter in processing data from null-point calorimeters.

4.8 The determination of surface heat flux as a function of time and temperature requires a digital computer, programmed to calculate the correct values of heat-transfer rate. Having the measured null-point cavity temperature, the problem to be solved is the inverse problem of heat conduction. Several versions of the well known Cook and Felderman numerical

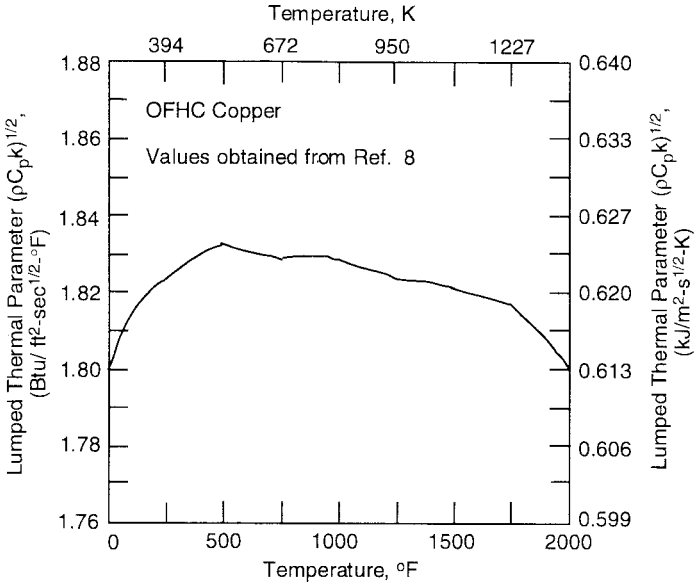

FIG. 6 Variation of $(\rho C_p k)^{1/2}$ with Temperature

integration equation **(9)** can be used to obtain the surface heat flux as a function of time. These equations are described in Section 10.

5. Significance and Use

5.1 The purpose of this test method is to measure extremely high heat-transfer rates to a body immersed in either a static environment or in a high velocity fluid stream. This is usually accomplished while preserving the structural integrity of the measurement device for multiple exposures during the measurement period. Heat-transfer rates ranging up to 2.84×10^2 MW/m^2 (2.5×10^4 Btu/ft^2-sec) **(7)** have been measured using null-point calorimeters. Use of copper null-point calorimeters provides a measuring system with good response time and maximum run time to sensor burnout (or ablation). Null-point calorimeters are normally made with sensor body diameters of 2.36 mm (0.093 in.) press-fitted into the nose of an axisymmetric model.

5.2 Sources of error involving the null-point calorimeter in high heat-flux measurement applications are extensively discussed in Refs **(3-7)**. In particular, it has been shown both analytically and experimentally that the thickness of the copper above the null-point cavity is critical. If the thickness is too great, the time response of the instrument will not be fast enough to pick up important flow characteristics. On the other hand, if the thickness is too small, the null-point calorimeter will indicate significantly larger (and time dependent) values than the input or incident heat flux. Therefore, all null-point calorimeters should be experimentally checked for proper time response and calibration before they are used. Although a calibration apparatus is not very difficult or expensive to fabricate, there is only one known system presently in existence **(6** and **7)**. The design of null-point calorimeters can be accomplished from the data in this documentation. However, fabrication of these sensors is a difficult task. Since there is not presently a significant market for null-point calorimeters, commercial sources of these sensors are few. Fabrication details are generally regarded as proprietary information. Some users have developed methods to fabricate their own sensors **(7)**. It is generally recommended that the customer should request the supplier to provide both transient experimental time response and calibration data with each null-point calorimeter. Otherwise, the end user cannot assume the sensor will give accurate results.

5.3 Interpretation of results from null-point calorimeters will, in general, be the same as for other heat-flux sensors operating on the semi-infinite solid principle such as coaxial surface thermocouples and platinum thin-film gages. That is, the effects of surface chemical reactions, gradients in the local flow and energy fields, thermal radiation, and model alignment relative to the flow field vector will produce the same qualitative results as would be experienced with other types of heat flux sensors. In addition, signal conditioning and data processing can significantly influence the interpretation of null-point calorimeter data.

6. Apparatus

6.1 In general, the null-point sensor shall consist of an OFHC copper hollow thick wall cylinder (closed on one end) with a fine wire thermocouple attached on the axial centerline in the bottom of the null-point cavity. The sensor assembly shall be configured to thermally simulate a semi-infinite solid in the time period of interest. The null-point cylinder will be flanged at the front and back to provide a thermally insulating air gap between the body of the sensor and the copper model as shown in Fig. 7. The sensor is normally installed in the model by press fitting. The null-point cavity radius-to-subsurface depth ratio *a/b*, shall be about (but not greater than) 1.4 **(6** and **7)**. The temperature sensor is usually a 0.508 mm (0.020 in.) diam stainless steel sheathed thermocouple wire with Chromel-Alumel (ANSI type K) thermoelements (0.102 mm; [0.004 in.] diam).

6.2 During data acquisition, the null-point calorimeter thermocouple output signal is recorded at a rate which will define the desired facility flow fluxuations. A common data sampling rate is 5000 points/sec with a 1 kHz analog filter. Data are normally recorded on disk file and can be transferred to another data storage medium. The raw analog data are normally smoothed before numerical integration techniques are employed to obtain the processed or reduced heat flux data. Discussions of smoothing techniques and numerical integration methods can be found in Refs **(6** and **7)**, respectively.

7. Experimental Time Response

7.1 It was shown by thermal analysis in Figs. 3 and 4 that proper time response was critical for the accurate use of null-point calorimeters in arc facility heat-flux measurement applications. Figs. 3 and 4 show that null point calorimeters can respond too quickly, thus indicating a significantly higher level than the actual heat flux incident upon the instrument's sensing surface. And, of course, null-point sensors can easily be too slow for the intended application. Therefore, the capability of performing experimental time response characterizations at high heat-flux levels in the laboratory is of vital importance. A prevailing misconception held by many users is that it is not possible to determine the actual time response of null-point sensors in the laboratory. Commercial suppliers of null-point calorimeters are presently unable to supply time response data with their sensors. Methods for obtaining null-point calorimeter experimental time response data have been developed for use at the Arnold Engineering Development Center (AEDC) and are documented in Refs **(6** and **7)**. The experimental data generally complement the analytical data, thereby enhancing the credibility of both methods.

7.2 A calibration system which was developed at the AEDC to experimentally determine the time response of null-point calorimeters uses a xenon arc lamp as the heat source and a fast response (5.1 m/sec) [200 in./sec] shuttering device. Fig. 8 shows graphical illustrations of experimental time response data obtained from a null-point sensor. These data were generated by irradiating a single null-point sensor with a high level (19.3 MW/m^2) constant heat flux from the xenon arc lamp very quickly with the fast shutter and recording the timewise output at 0.2-m/sec time intervals. The timewise output was converted to a temperature history by applying the appropriate equations for a type K thermocouple. As shown in Fig. 8, the null-point cavity temperature increased by nearly 97 K (175°F) in less than 30 m/sec. The resulting timewise heat

TYPICAL DIMENSIONS		
	mm	in.
a	0.318	0.0125
b	0.229	0.009
c	0.102	0.004
d	2.03	0.080
D	2.36	0.093
L	10.2	0.400
R_B	6.35	0.250

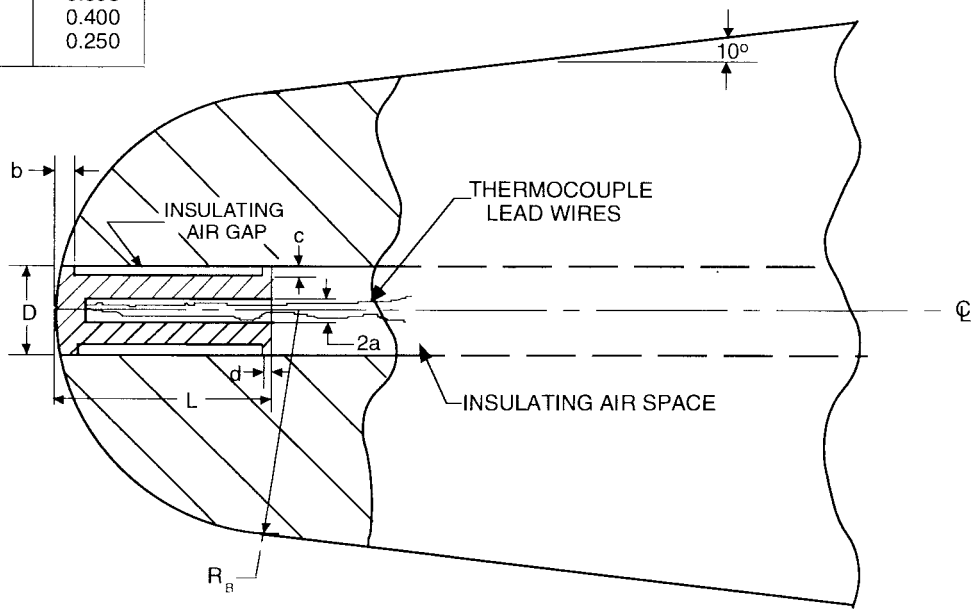

FIG. 7 Typical Null-Point Calorimeter Installation

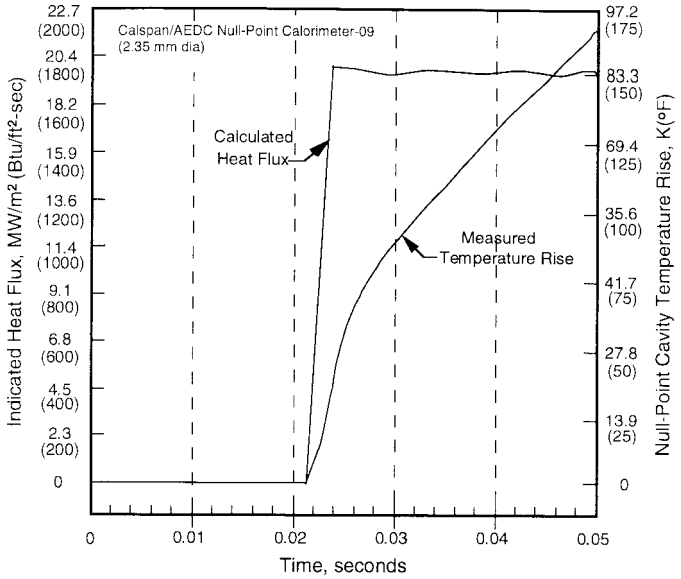

FIG. 8 Null-Point Calorimeter Experimental Time Response Data

flux on Fig. 8 was obtained by inserting the temperature history into (Eq 1) and applying the room temperature thermal properties of OFHC copper. A time response of 3 to 4 m/sec to full scale output is indicated by the timewise heat-flux data. These data represent near optimum sensor behavior. If the copper foil thickness above the null-point cavity was thinner, operating behavior such as exhibited by the thin sections on Figs. 3 and 4 probably would have resulted.

8. Calibration

8.1 Thermal analyses of the null-point concept show that small changes in physical dimensions of null-point sensors can cause significant differences in calibration. Therefore, all null-point calorimeters should be experimentally calibrated at high heat-flux levels in the laboratory before using them in a severe aerothermodynamic test environment. With equipment currently available, a maximum heat flux of approximately 22.7 MW/m^2 (2000 Btu/ft^2-sec) exists for performing laboratory calibrations **(6** and **7)**. This calibration heat source system was designed to provide a heat flux high enough to approximate the low to medium levels experienced in an arc heater facility flow, but not high enough to damage the sensors (by ablation) during the calibration period. This hardware was also designed to have a high degree of versatility in that single units can be calibrated in the laboratory before installation in the test model and also calibrated after installation in a test model. By calibrating null-point sensors before installation, a sensor with slow time response and low output can be machined to remove a small bit of material from the surface and bring them into calibration tolerance before installation.

8.2 The heat source for the high heat flux calibration system is a 1.6 kW xenon arc lamp optically focused onto a relatively small area and powered by a pulsed 6 kW power supply. An optical integrator is employed with the system to provide a uniform area of heat flux about 6.35 mm (0.25 in.) diam at the focal plane. The calibration standard is a commercial Gardon gage whose calibration is traceable to a blackbody oven source. The temperature of the blackbody source is measured by an

optical pyrometer certified by NIST through application of the Stefan-Boltzmann equation **(10)**.

8.3 A thin (≤0.0127 mm [0.0005 in.]) coating of high absorptivity must be applied to the sensing surface of each null-point sensor and standard alike to perform accurate heat-flux transducer calibrations. This coating must be capable of withstanding relatively high temperatures (>811 K [1000°F]) in this transient measurement application. After screening several candidate coatings, Krylon High Heat Spray Paint #611260 was chosen as the standard coating in this application because of the ease of application, high temperature capability, high absorptivity (0.95), and availability.

8.4 With modern data acquisition and processing equipment available even for laboratory experiments, the timewise thermocouple output signal is amplified and stored on disk file. It is then converted to sensor temperature rise and processed into indicated heat flux units by a numerical integration computer program. These data are available in tabular and plotted format less than five minutes after the data run.

8.5 Plasma arc facilities have been used as a heat source to calibrate null-point calorimeters by comparing the null-point heat flux output to that of a standard heat-flux gage or a circular foil calorimeter. Because of the high degree of uncertainty in the repeatability of the arc and its frequency content, this method is not recommended as a means of null-point calorimeter calibration.

9. Procedure

9.1 In the past null-point calorimeters were utilized in what is termed the "destruct mode" of operation. When used in this manner, the model with the null-point sensor installed is injected into the test environment and brought to rest. For convective heat transfer measurements, a TFE-fluorocarbon cap is used to protect the null-point sensor during insertion. The cap ablates after a short time period and exposes the sensor during insertion. The cap ablates after a short time period and exposes the sensor to the high energy environment. When this mode of operation is employed, the sensor and the model in which it is installed are usually damaged by ablation (melting). This "destruct mode" of testing is no longer recommended because of the expense and uncertainty involved.

9.2 The procedural method now commonly used is to sweep the test model containing the null-point calorimeter through the test environment at a rate consistent with the sensor time response and time-to-burnout. Starner **(11)** suggested the swept mode, and it was further developed by Kennedy, Rindal, and Powers **(4** and **5)**. Using the swept mode of operation, numerous measurements (up to 50) can be made with the same calorimeter probe—certainly a more economical use than the "destruct mode."

10. Calculation of Heat Flux

10.1 Calculation of heat transfer rates from null-point calorimeter output signals involve the use of equations based upon semi-infinite solid heat conduction. The classical equation relating the incident heat flux, $\dot{q}$ (t), in terms of the timewise surface temperature, $T(t)$, is given by **(9)**:

$$q(t) = \frac{(\rho C_p k)^{1/2}}{\pi^{1/2}} \left[\frac{T(t)}{t^{1/2}} + 1/2 \int_0^t \frac{T(t) - T(\tau)}{(t-\tau)^{1/2}}\, d\tau \right] \tag{1}$$

where ρ, C_p, k, and τ are density, specific heat, thermal conductivity, and a dummy variable of integration, respectively. Reduction of heat flux data was a formidable problem for the users of surface temperature measuring devices such as the platinum thin film resistance thermometer and the coaxial surface thermocouple until the mid-1960s because the timewise output from the sensors cannot be represented by a simple analytical expression. However, in 1966 Cook and Felderman **(9)** developed a numerical expression for the heat flux whereby the temperature-time curve was approximated by a piece-wise linear function over a number of small, equal time increments. This expression involved no integration approximations and the accuracy of the result was limited only by the degree to which the true input function is represented by a piece-wise linear expression. The numerical equation developed by Cook and Felderman is shown below as (Eq 2):

$$\dot{q}(t) = \frac{(\rho C_p k)^{1/2}}{\pi^{1/2}} \left[\frac{T(t)}{t^{1/2}} + \frac{T(t) - T(\tau - \Delta t)}{\Delta t^{1/2}} + \sum_{i=1}^{n-1} \left(\frac{T(t) - T(t_i)}{(t - t_i)^{1/2}} - \frac{T(t) - T(t_{i-1})}{(t - t_{i-1})^{1/2}} + 2\frac{T(t_i) - T(t_{i-1})}{(t-t_i)^{1/2} + (t-t_{i-1})^{1/2}} \right) \right] \tag{2}$$

10.1.1 Although the development of (Eq 2) represented a major breakthrough in the processing of heat-flux data from surface temperature measuring devices, it is a rather cumbersome expression to program for calculations on a digital computer. Therefore, several short form versions of this expression have been derived since the publication of the original article **(9)**. A short form version of (Eq 2) developed by Don Wagner of Sverdrup Technology in 1974 is shown as (Eq 3) below:

$$\dot{q}(t) = \frac{2(\rho C_p k)^{1/2}}{\pi^{1/2}} \sum_{i=1}^{n} \frac{T_i - T_{i-1}}{(t_n - t_i)^{1/2} + (t_n - t_{i-1})^{1/2}} \tag{3}$$

The expression above is routinely used in the reduction of heat flux data in several arc facilities at the present time. Of course, (Eq 3) is easily programmed for repetitive calculations on a digital computer. Calculations of heat flux data using (Eq 3) are preceded by smoothing the timewise temperature data. Normal smoothing of timewise temperature is accomplished by the sectional fitting of a second order polynominal and applying the least squares method. However, a new technique has been developed for the temperature data in the arc facilities at the AEDC. This new technique is an adaptation of the least squares method, but involves only a selected number of data points near the end of the useful run time. The number of data points over which the smoothing technique is applied is dependent upon the amount of noise in the data.

10.1.2 Fig. 9 is a graphical illustration of typical smoothed timewise temperature and heat-flux data obtained at the stagnation point of a 12.7 mm (0.5 in.) diam, 10-degree half angle sphere cone standard probe in arc heater H1 at the AEDC **(7)**. The sensor was a 2.36-mm (0.093-in.) diam copper null-point calorimeter. Although the null-point cavity temperature reached about 756.7 K (1330°F) during the run duration, it did

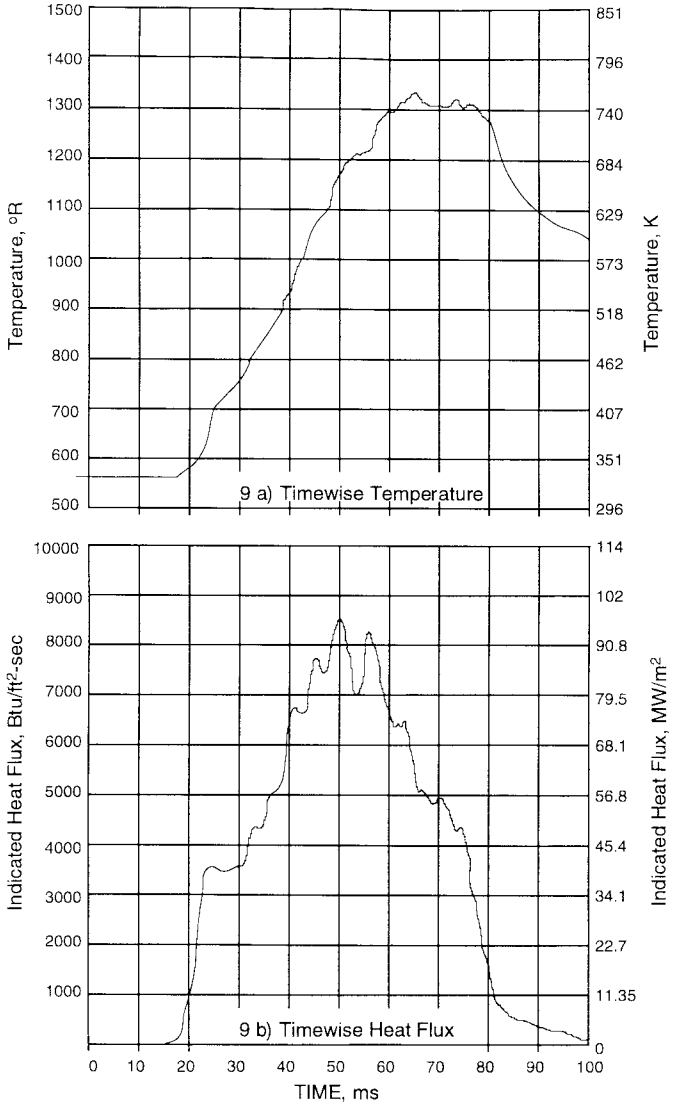

FIG. 9 AEDC Arc Heater Null-Point Probe Data

not come close to the melting point of copper which is 1356 K (1981°F). These raw temperature data were recorded at 5000 points/sec with a critically damped, two-pole 1 kHz analog filter in front of a dc amplifier.

10.2 Also required for obtaining accurate heat-flux data is a knowledge of the lumped thermal property parameter, $(\rho C_p k)^{1/2}$, defined in the previous section. Thermal properties of OFHC copper are known to good accuracy up to temperatures approaching the melting point, 1356 K. The variation of $(\rho C_p k)^{1/2}$ for copper is not a strong function of temperature, rising only 2–3 percent from room temperature to the melting point. This variation was taken from Ref **(8)** and is graphically shown in Fig. 6. This small change in $(\rho C_p k)^{1/2}$ with temperature leaves the null-point calorimeter user with a choice of either programming the variation into the data reduction equation or ignoring it because it is not a major contributor to the accuracy of the final data.

11. Report

11.1 In reporting the results of null-point calorimeter measurements, the following should be noted:

11.1.1 Test environment,

11.1.2 Reservoir (stagnation conditions, or radiant heat source conditions, or both),

11.1.3 Test section conditions,

11.1.4 Model geometry and surface conditions,

11.1.5 Dimensions and material of null-point calorimeter,

11.1.6 Null-point calorimeter temperature versus time data,

11.1.7 Calculated heat-transfer rate versus time data.

11.1.8 Type of heat flux data processing program used, and

11.1.9 Raw temperature data smoothing technique used.

12. Keywords

12.1 calorimeter; convective; heat flux; heat flux gage; null-point; radiative; transient temperature

REFERENCES

(**1**) Masters, J. I., and Stein, S., "Effects of an Axial Cavity on the Temperature History of a Surface Heater Slab," *The Review of Scientific Instruments*, Vol 27, No. 12, December 1956, pp. 1065–1069.

(**2**) Beck, J. V., and Hurwicz, H., "Effects of Thermocouple Cavity on Heat Sink Temperature," Transactions of the ASME—Journal of Heat Transfer, Vol 82, No. 1, February 1960, pp. 27–36.

(**3**) Howey, D. C., and DiCristina, V.," Advanced Calorimetric Techniques for Arc Plasma Heat Transfer Diagnostics in the Heat Flux Range up to 20 kW/cm^2," AIAA Paper No. 68-404, presented at the AIAA 3rd Aerodynamic Testing Conference, April 8–10, 1968.

(**4**) Kennedy, W. S., Rindal, R. A., and Powars, C. A.," Heat Flux Measurement Using Swept Null Point Calorimetry," AIAA Paper No. 71-428, presented at the AIAA 6th Thermophysics Conference, April 26–28, 1971.

(**5**) Powars, C. A., Kennedy, W. S., and Rindal, R. A., "Heat Flux Measurement Using Swept Null Point Calorimetry," *Journal Spacecraft*, Vol 9, No. 9, September 1972, pp. 668–672.

(**6**) Kidd, C. T., "Recent Developments in High Heat-Flux Measurement Techniques at the AEDC," Proceedings of the 36th International Instrumentation Symposium, May 1990, pp. 477–492.

(**7**) Kidd, C. T., "High Heat-Flux Measurements and Experimental Calibrations/Characterizations," NASA CP-3161, September 1992, pp. 31–50.

(**8**) Touloukian, Y. S., "Thermophysical Properties of High Temperature Solid Material, Vol 1: Elements," Thermophysical Properties Research Center, Purdue University, 1966.

(**9**) Cook, W. J., and Felderman, E. J., "Reduction of Data from Thin-Film Heat-Transfer Gages: A Concise Numerical Technique," AIAA Journal, Vol 4, No. 3, March, 1966.

(**10**) Carslaw, H. S., and Jaeger, J. C., *Conduction of Heat in Solids*, Clarendon Press, Oxford, 1959 (Second Edition).

(**11**) Starner, K. C., "Use of Thin-Skinned Calorimeters for High Heat Flux Arc Set Measurements," ISA Preprint No. P-11-5- PHYMMID-67, presented at 22nd Annual ISA Conference and Exhibit, Sept. 1967.